

**FACTORS CONTROLLING WHICH CRATERS DEVELOPED INLET VALLEYS ON EARLY MARS.**

Emily R. Bamber<sup>1, 2</sup>, T. A. Goudge<sup>1, 2, 3</sup>, C. I. Fassett<sup>4, 5</sup>, G. R. Osinski<sup>6</sup>, G. Stucky de Quay<sup>7</sup>. <sup>1</sup>Department of Geological Sciences, Jackson School of Geosciences, The University of Texas at Austin, Austin, TX, USA; <sup>2</sup>Center for Planetary Systems Habitability, The University of Texas at Austin, Austin, TX, USA; <sup>3</sup>CIFAR Azrieli Global Scholars Program, CIFAR, Toronto, Ontario, Canada; <sup>4</sup>Johns Hopkins Applied Physical Laboratory, MD, USA; <sup>5</sup>Department of Earth Sciences, University of Western Ontario, London, ON, Canada; <sup>6</sup>Department of Earth, Atmospheric, and Planetary Sciences, Massachusetts Institute of Technology, Cambridge, MA, USA.

**Introduction:** Impact crater degradation, including reduction of rim relief and denudation of ejecta blankets, was active on early Mars [e.g., 1-3]. Many degraded impact craters with low rim relief also have inlet valleys [4, 5]. Previously we found that the crater rim removal accomplished during degradation on early Mars may have prepared craters for inlet incision during the valley network (VN)-forming era [5]. However, not all rimless craters on Mars have inlets, so degradational rim removal could not have been the only control on VN inlet formation. In this study, we ask: Why were some, but not all, low-rimmed craters breached during the VN-forming era? To answer this, we test whether there are any measurable distinctions between VN-breached and non-breached degraded Noachian craters. A full explanation of the methods, results and discussion detailed here is available in [13].

**Hypotheses:** All else being equal, we hypothesize that inlet formation was promoted for craters: (i) on longer and steeper slopes; (ii) with larger catchments, (iii) with greater local VN drainage densities; and (iv) that are more deeply inset into the landscape. We also hypothesize that terrain roughness and rim topographic variability may have had an effect on inlet formation. Other features (erodibility, climate variations) may have played a role, but we do not test them here.

**Approach:** We evaluated the topography and hydrology around 103 degraded impact craters, 51 with and 52 without VN inlets, between 40°N and 40°S, with diameters 12-150 km. VN-breached degraded craters were selected from catalogs of martian paleolakes [4, 5]. Non-breached craters, in the S. highlands within 100 km of a VN and other paleolakes, were selected from a catalog of martian craters [6].

**Topography.** We used products derived from MOLA elevation to measure slope and roughness. A clip of the spherical harmonic model (SHM) of Mars' topography up to degree 20 (~500 km on Mars) [7] was extracted at each circular buffer distance and used to calculate the regional slope. A "sector" 60° either side of the upslope orientation was mapped for each buffer distance ("upslope sector"). Median differential slope (MDS) maps [8] were clipped to each sector buffer area, and the median value of MDS serves as the regional roughness metric. Roughness was assessed at 0.6, 2.4, and 9.2 km baseline length scales.

Where CTX and HRSC DEMs were available, we mapped the along-rim profile within the upslope sector and evaluated crater rim topographic variability following [8], with MDS calculated for baseline length scales of: 25 m, a tenth of the crater radius, and 0.6, 1.0, 2.4, 10.0 and 19.2 km.

**Hydrology.** To measure the catchment area from which runoff, if present, would contribute to the crater (potential contributing area), we calculated flow accumulation maps from MOLA elevation, and measured the upstream watershed area from selected pour points using ArcMap's hydrology tools. Breached craters' pour points are the point of highest flow accumulation at one crater radius from the crater center and within an inlet valley. Non-breached craters' pour points are the point of highest flow accumulation outside the crater and within 1.25 R of the crater center.

We estimated VN drainage density (VN length per area) for each buffer distance. To avoid bias due to the presence of the required inlet valley around breached craters, we calculated drainage density over the circular buffer area excluding the upslope sector (where the inlet is usually located) and crater interior. Valley length was estimated from the map of VNs by [9], excluding all non-VN valley types.

Lastly, we calculated an inset index,  $I$ :

$$I = (\text{mean } Z \text{ upslope} - \text{min } Z \text{ inside crater}) / \text{crater depth}$$

Where  $Z$  is absolute elevation.  $I$  is a dimensionless factor which quantifies the number of crater depths ( $d$ ) the crater floor is below the average upstream terrain. We suggest a deeply inset crater (high  $I$  value), is likely to be a strong regional sink for water, versus a crater relatively perched above the surrounding terrain, which might receive limited water.

**Results: Topography.** The magnitude of regional slope does not differ significantly between breached and non-breached craters (mean = 0.0036 m/m and 0.0035 m/m respectively; Figure 1A). These slope values are high compared to Earth's river slopes [11]. Breached and non-breached craters also have similar surface roughness (Figure 1B) and median differential slope values of the along-rim topographic profile, representing rim topographic variability. This holds for all baseline length scales. The lack of divergence in topographic metrics between breached and non-breached

craters is contrary to our initial hypotheses, but consistent with previous modeling [10].

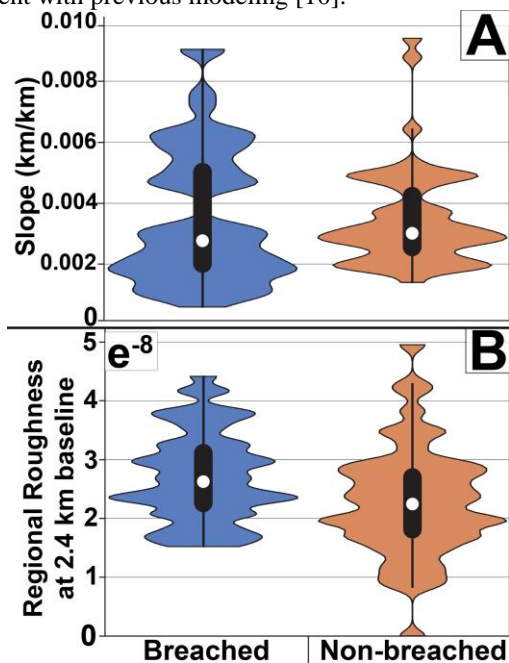


**Figure 1:** Violin plots for regional slope magnitude (a), and roughness at the 2.4 km baseline length (b), split by breached (left,  $n=51$ ) and non-breached (right,  $n=52$ ). White circle: median; Bold black line: upper and lower quartiles; thin black vertical line: range of non-outlier data; solid violin: kernel density estimation of whole distribution.

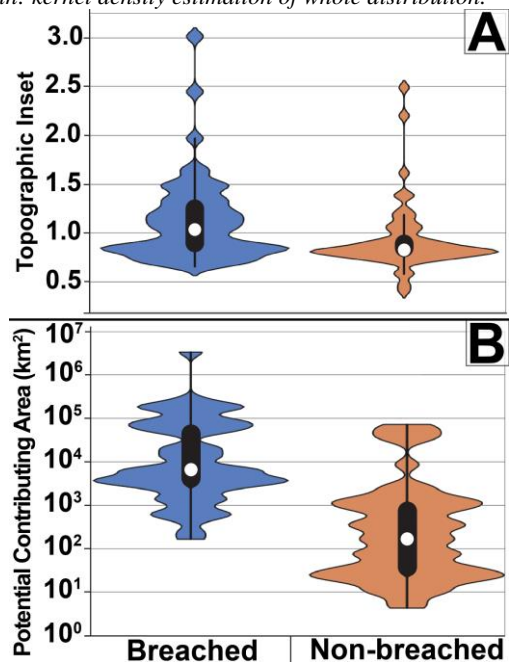


**Figure 2:** Violin plots for topographic inset ( $I$ ) (a), and potential contributing area (note the log y scale) (b), split by breached (left,  $n=51$ ) and non-breached (right,  $n=52$ ). See Figure 1 caption for plot details.

**Hydrology.** The  $I$  value distribution for breached craters is broader and skewed to higher values than non-breached craters (Figure 2A). There is a greater than twenty-fold difference in the measured potential contributing area between breached ( $\sim 1.1 \times 10^5$  km<sup>2</sup>) and non-breached craters ( $\sim 5.3 \times 10^3$  km<sup>2</sup>) (Figure 2B). There is also a large difference in the mean and distribution of VN drainage density for breached (0.0230 km/km<sup>2</sup>) versus non-breached (0.0127 km/km<sup>2</sup>) craters (which is even more pronounced for areal limits closer to the crater center).

**Discussion:** In contrast to the topographic metrics, hydrologic metrics are very different between breached and non-breached craters (Figure 2). We suggest this demonstrates that slope and surface roughness typically surpassed any thresholds for VN incision on Mars, making hydrologic factors the limiting control on whether incision was possible.

Features that we are not able to measure, such as variations in climate or hydrological conditions (e.g., permeability, subglacial melt production) may explain the observed hydrologic differences between breached and non-breached craters. However, breached craters are also more deeply inset into the landscape. Such deeply inset craters likely acted as regional sinks for water, and hampered fluvial activity (i.e., inlet formation) around nearby, less inset craters. The observed importance of inset is likely a consequence of Mars' dominantly impact-generated relief structure, where craters segregate the landscape into disconnected basins that hinder fluvial connectivity [e.g., 3, 7, 9, 12].

**Acknowledgments:** This was supported by a NASA MDAP grant, and a NASA FINESST grant to Bamber. We thank B. A. Black for sharing MOLA SHM data [7] and S. J. Robbins for supplying the catalog of craters >1 km on Mars [6].

**References:** [1] Craddock, R. A., & Howard, A. D. (2002). *JGR*, 107(E11); [2] Forsberg-Taylor, N. K. (2004). *JGR*, 109(E5), E05002; [3] Matsubara, Y., et al. (2018). *JGR*, 123(11), 2958–2979; [4] Goudge, T. A., et al., (2016). *Geology*, 44(6), 419–422; [5] Bamber, E. R., et al., (2022). *Icarus*, 378, 114945; [6] Robbins, S. J., & Hynes, B. M. (2012). *JGR*, 117(E6); [7] Black, B. A., et al., (2017). *Science*, 356(6339), 727–731; [8] Kreslavsky, M. A., & Head, J. W. (2000). *JGR*, 105(E11), 26695–26711; [9] Goudge, et al., (2021). *Nature*, 597(7878), 645–649; [10] Enns et al., (2010). *LPSC*, #2065; [11] Cohen et al., (2018). *J. Hydrology*, 563, 1057–1067; [12] Irwin, R. P., et al., (2011). *JGR*, 116(E2), E02005. [13] Bamber, E. R., et al., (2023). *GRL*, 49, e2022GLI01097.